Progress in Joule-Thomson Microcooling at the University of Twente

J.H. Derking[1], D.W. Zalewski[1], M. Garcia[1], H.J. Holland[1], A.V. Mudaliar[1], H. Cao[1], P.P.P.M. Lerou[2], and H.J.M. ter Brake[1]

[1]University of Twente, Faculty of Science and Technology,
7500 AE Enschede, The Netherlands
[2]Kryoz Technologies,
7521 PV Enschede, The Netherlands

ABSTRACT

The development of miniaturized Joule-Thomson (JT) coolers has been an ongoing research topic at the University of Twente for many years. In the current research, a new run of single-stage JT microcoolers with gross cooling powers of 40 mW and 180 mW at 100 K was developed and fabricated. The temperature profiles along the counter-flow heat exchangers of both types were measured, as were their net cooling powers. Operated with nitrogen gas, the latter was measured to be 26 mW at 90 bar and 131 mW at 80 bar, for both types, respectively. Furthermore, it is shown that the influence of gravity on the performance of the microcoolers is negligible.

Also, the issue of clogging caused by tiny amounts of water is further investigated. No clogging is observed when the microcooler is driven by gas cleaned with a microtorr® getter filter. However, when unpurified gas is used, clogging occurs during cool down and prevents the microcooler from cooling down below about 230 K.

Furthermore, the incorporation of sorption compressors is explored to make a closed-cycle JT microcooler that delivers 50 mW at 100 K. A final design is made on the basis of a quasi-static thermodynamic analysis. The cooler will operate with methane as the working fluid, and the total input power will be around 33 W.

INTRODUCTION

Micromachined Joule-Thomson (JT) coolers have been investigated at the University of Twente for many years.[1-3] The cold stage of the microcoolers consist of a stack of three glass wafers. The high and low-pressure lines are etched as rectangular channels with supporting pillars in the top and bottom wafer. The high-pressure line ends in a flow restriction, which is connected to the low-pressure line, thereby forming a counter-flow heat exchanger (CFHX) between the high and low-pressure channel. A thin layer of gold is sputtered on the outer surface to minimize the parasitic heat loss due to radiation. Operated with nitrogen gas, at a high pressure of 80 bar and a low pressure of 6 bar, typical net cooling powers of 10-20 mW at 100 K were obtained.[3] The cold stages were optimized for maximum performance in combination with

Cryocoolers 16, edited by S.D. Miller and R.G. Ross, Jr.

minimum dimensions.[4] Typical dimensions of a cold stage with a net cooling power of 10 mW at 100 K are 30 x 2.2 x 0.7 mm.

The current research is focused on developing JT microcoolers with higher net cooling powers (up to 200 mW) and the incorporation of sorption compressors. Furthermore, the utilization of JT microcoolers is explored in pilot projects, such as cooling of low-noise amplifiers or optical detectors. Also, the issue of clogging caused by tiny amounts of water is further investigated. To reach lower temperatures, multi-stage microcoolers are investigated. A separate paper on this topic is presented elsewhere in this proceedings.[5] In the present work, the recent developments in the Twente microcooling research on single-stage microcoolers are discussed.

SINGLE-STAGE JOULE-THOMSON MICROCOOLERS

In 2009, a new run of microcoolers was developed and fabricated consisting of two types of single-stage JT microcoolers: one with a gross cooling power around 40 mW and one with a gross cooling power around 180 mW at 100 K at a high pressure of 80 bar. All dimensions of both microcoolers are equal except the restriction dimensions. Measurements were done to characterize both types and the results are discussed in this section.

During the measurements, nitrogen gas (5.0) is supplied from a pressurized gas bottle. A microtorr® getter filter from Saes Pure Gas Inc.[6] is used to remove most impurities (especially water) from the gas to a parts-per-trillion level. The connections from the gas tubes to the microcooler are made with indium seals. The microcooler is placed into a vacuum flange and mounted in a vacuum chamber in which a vacuum pressure of less than $1x10^{-5}$ mbar is maintained. The pressures and mass-flow rates of the incoming and outgoing gas streams are measured. As temperature sensors, platinum resistors (Pt1000) are used, which are glued to the microcooler with conductive silver glue. The error in the temperature measurements is around 1 K. Aluminum bond wires with a diameter of 25 µm are used to make the electrical connections from the sensors to a printed circuit board (PCB) that surrounds the JT microcooler. Standard surface-mounted-device (SMD) resistors are used as heaters.

High Cooling Power JT Microcooler

The temperature profile along the length of the CFHX is measured by seven temperature sensors that are glued on top of the low-pressure side of the JT microcooler. Furthermore, an SMD resistor is glued to the cold-tip that is used as a heater for measuring the cooling power. Fig. 1 shows the microcooler mounted in a vacuum flange and surrounded by a PCB. Also, the location of the sensors and heater is indicated as well as the numbering of the sensors used throughout the paper. The JT microcooler is operated with nitrogen gas at a high pressure of 80 bar and a low pressure of 6 bar.

In Fig. 2, the measured temperatures and mass-flow rate versus time are given. The cold-tip cools down from 290 K to 101 K in less than 7 minutes. During the cool-down phase, the mass-

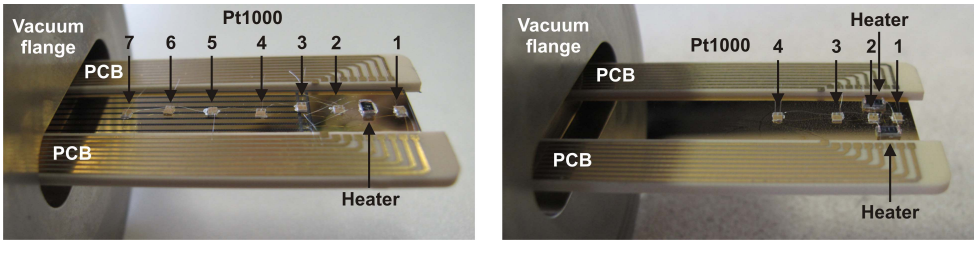

Figure 1. Photographs of JT microcoolers mounted into a vacuum flange and surrounded by a PCB. The location of the temperature sensors and the heaters is indicated. The numbering of the temperature sensors starts at the cold tip. Aluminum bond wires are used to make the electric connections between sensors and PCB. Left: high cooling power JT microcooler and right: low cooling power JT microcooler.

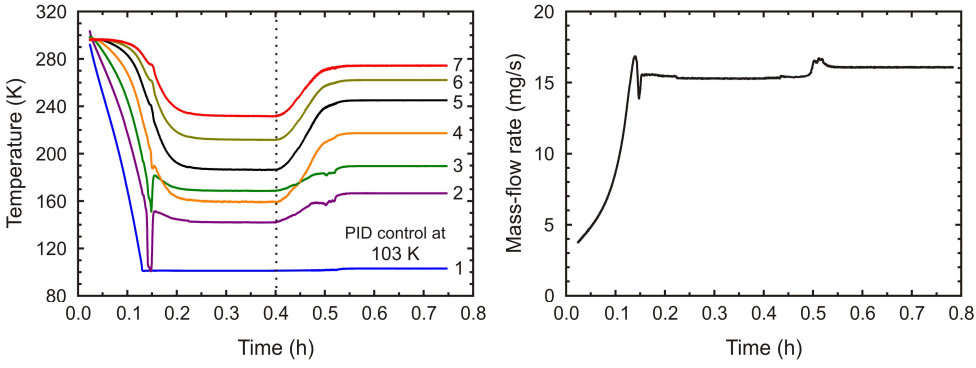

Figure 2. Measurement results of the high cooling power JT microcooler. Left: Temperature versus time measured by seven sensors along the CFHX. The location of the sensors on the microcooler is indicated in Fig. 1. Right: mass-flow rate versus time.

flow rate increases from 4 to 17 mg/s, and after cool down it becomes stable at 15.6 mg/s. A finite volume model made in Ansys Fluent[7] is used to calculate the pressure drop in the low-pressure channel. This pressure drop depends on the mass-flow rate and is calculated to be around 2 bar, resulting in a pressure of 8 bar in the evaporator. That pressure corresponds to a saturated liquid temperature of 100.4 K, very well matching the measured temperature.

Shortly after the cold-tip reaches 101 K, the second sensor also measures this temperature for a few seconds, but then heats up again. Also, in all other temperature sensors, a change in reading can be observed at the same time. The mass-flow rate at this time reaches its maximum value and decreases steeply, resulting in a decrease in cooling power. Most probably this change in mass-flow rate causes the change in reading of all temperature sensors. Furthermore, before all sensors reach a stable temperature, the fourth sensor measures a lower temperature than the third one. Also, there is a temperature gradient of about 40 K between the first and the second sensor. It was expected that an isothermal two-phase region forms in the evaporator. The two-phase flow also partly fills the return of the CFHX until there is a heat balance between the loss due to CFHX inefficiency and the available cooling power.

This particular microcooler has electrical leads that were structured into the gold layer with uncovered parts of glass in between. This makes it possible to look inside the CFHX while the microcooler is operating. With no heater power supplied, one can see liquid droplets moving with a high speed into the CFHX. This behavior was observed before by Lerou et al.[8] when investigating clogging in JT microcoolers. This effect indicates that no two-phase region is formed in the evaporator. Most probably, liquid droplets flow into the CFHX where they evaporate and in this way cool down the CFHX, resulting in temperatures of all sensors that are much lower than expected. This can also be the reason that the fourth sensor has a lower temperature than the third one.

By placing temperature sensor one and the heater resistor in a PID control loop, the temperature of the cold-tip can be controlled. This is done for a cold-tip temperature slightly higher than the saturated liquid temperature, meaning that all formed liquid is evaporated. The resulting temperature profile is also shown in Fig. 2. In this case, all measured temperatures are in increasing order from the cold to the warm end of the CFHX. Also, all measured temperatures are much higher than in the case where no heater power is supplied. The net cooling power of the JT microcooler corresponds to the supplied heater power, which in this situation is around 131 mW. Using a thermal mathematical model made in ESATAN[9] to calculate the performance of the microcooler, results in a calculated cooling power of 182 mW. In this model, losses due conduction through the CFHX material and radiation to the environment are taken into account. The loss due to conduction through the wiring of the sensors is calculated to be 16 mW, resulting in a calculated net cooling power of 166 mW. The difference of 35 mW between calculated and

measured cooling power can be caused by an increase in radiative heat load due to, for example, moisture on the outside of the microcooler. Another reason can be that the conduction loss through the wiring of the sensors is higher than calculated.

To investigate the effect of gravity on the performance of the JT microcooler, it is operated in different orientations (for example, tipped down or up). The measurements show no big deviations from the performance of the microcooler in horizontal orientation. Mass-flow rates and cool-down times are equal, as well as the final temperatures of all sensors. Therefore, it is concluded that gravity has no influence on the performance of the microcooler.

Low cooling power JT microcooler

To see whether the above-described effects also occur in microcoolers with lower cooling powers and hence lower mass-flow rates, the temperature profile is also measured along the length of the CFHX of a lower-power microcooler. Now, four temperature sensors are glued on top of the low-pressure side of the JT microcooler. Two heating SMD resistors are placed in series to distribute the applied heat more evenly over the cold tip. The location of the sensors and the heaters are given in Fig. 1. The microocooler is operated with nitrogen gas at a high pressure of 90 bar and a low pressure of 6 bar. Fig. 3 shows the measured temperatures as well as the mass-flow rate versus time.

The measured cool-down time from 300 K to 96.3 K is around 90 minutes. During the cool-down phase, the mass-flow rate increases from 1 to 4.2 mg/s and after cool down it becomes stable at 3.4 mg/s. The calculated pressure drop corresponding to this mass-flow rate is around 400 mbar. The pressure in the evaporator is thus 6.4 bar, which corresponds to a saturated liquid temperature of 97.3 K, matching the measured temperature within measuring accuracy.

As in the high-power microcooler, one can see a drop in the second sensor reading directly followed by an increase in temperature coinciding with a peak in the mass-flow rate. Furthermore, there is a temperature gradient of 14 K between the first and second sensor. Also, a big fluctuation in the temperature of the second sensor can be observed as well as a somewhat smaller fluctuation in the temperature of the third sensor.

Again, the first sensor is PID controlled at a temperature slightly above the saturated liquid temperature. The temperature profile in this situation is also given in Fig. 3. As can be seen, all measured temperatures significantly increase compared to the situation where no heater power is applied. When the tip is controlled at 101 K, the measured cooling power is around 26 mW. Simulations show that the calculated cooling power is around 53 mW. The heat load due to conduction through the wiring of the sensors is calculated to be 14 mW, resulting in a calculated net cooling power of 39 mW. Again, the difference of 13 mW can be explained by an increased radiative heat load.

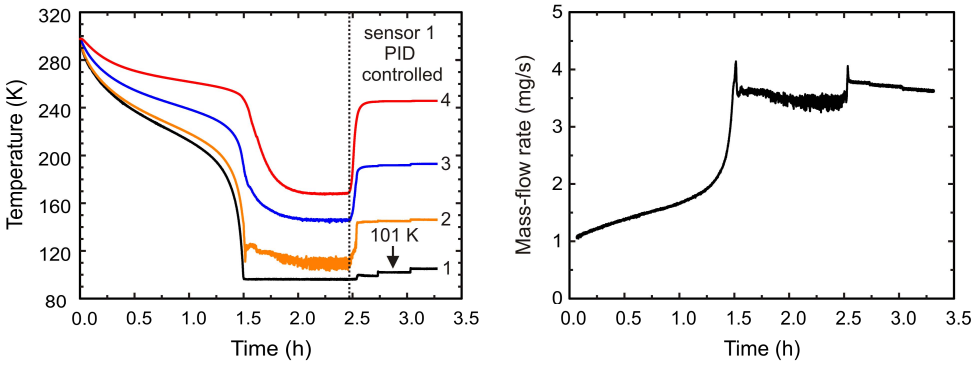

Figure 3. Measurement results of the low cooling power JT microcooler. Left: Temperature of four sensors placed along the CFHX versus time. The location of the sensors is shown in Fig. 1. Right: mass-flow rate versus time.

CLOGGING

The performance of JT microcoolers is constrained due to the deposition of small amounts of water inside the microcooler. Ice crystals form a congestion in or in front of the restriction, resulting in a decrease in mass-flow rate and hence in cooling power. Clogging in very small JT microcoolers was already investigated by Lerou et al.[8] In the current microcoolers, we expect less effect of clogging, because these have larger restriction dimensions (larger cooling powers). Measurements were performed in this respect on the 40 mW gross microcooler.

Two different experiments were conducted: the first one without a microtorr® getter filter[6] in the high-pressure gas flow, and the second one using such a filter. The mass-flow rates versus cold-tip temperature of both experiments are shown in Fig. 4. In the left part of the figure, which gives the result without using the getter filter, the mass-flow rate decreases around 230 K indicating clogging of the restriction. As the mass-flow rate drops, so does the cooling power, and the temperature of the cold tip increases. Around 238 K, the mass-flow rate increases again, but to a lower level than during the first cool down. This indicates that some of the ice that blocked the restriction has sublimated and passed the restriction. Due to the increase in cooling power, the cold-tip starts to cool down again, but only to about 235 K. There, the cycle of clogging and declogging starts again until some kind of equilibrium is reached where the amount of ice that is formed is impeding the mass-flow rate in such a way that the cooling power is equal to the parasitic heat flux. The microcooler does not cool down further.

By using the getter filter, the water contamination in the nitrogen gas is reduced to approximately 250 parts per trillion. The right part of Fig. 4 gives the mass-flow rate versus the cold-tip temperature in the case that the getter filter is used. As shown, the mass-flow rate increases from 1 to 4 mg/s during cool down without showing a sign of clogging. When the cold-tip reaches 98 K the mass-flow rate first increases and then decreases to a minimum value of around 3.1 mg/s. This change of mass-flow rate is caused by a change in restriction temperature. After running the JT microcooler for approximately 12 hours the cold-tip starts to warm up spontaneously. Initially, no hysteresis is observed in the mass-flow rate versus cold-tip temperature graph. This indicates that the warming up is not caused by clogging, because in that case a decrease in mass-flow rate should be measured. Most probably, the microcooler warms up due to the deposition of moisture on the outside of the microcooler. This decreases the effectiveness of the gold coating, resulting in an increase in radiative heat load.

During the warming up of the microcooler, at around 200 K a sharp decrease in mass-flow rate is observed. This is an indication that clogging of the restriction occurs. It is expected that during the cool-down phase, ice crystals grow inside the CFHX at a local temperature of around 200 K (corresponding to a partial water pressure of 1 Pa). During the warming up, the phase transition zone shifts towards the cold tip.[8] Since the mass-flow rate decreases significantly it

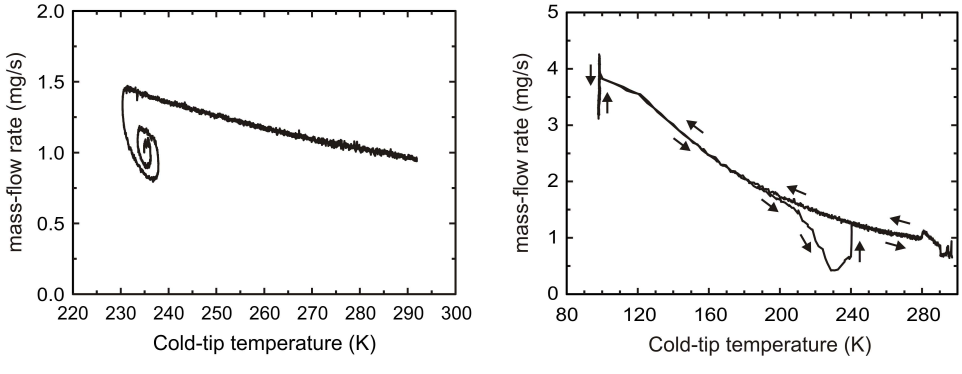

Figure 4. Mass-flow rate versus cold-tip temperature of the low power JT microcooler. Left: Cool down when unpurified nitrogen gas (5.0) is used to drive the microcooler. Right: high pressure nitrogen gas has been cleaned with a microtorr® getter filter before it enters the microcooler.

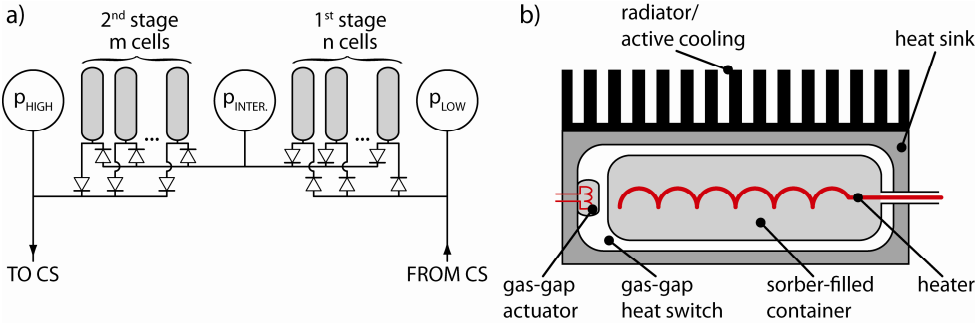

Figure 5. a) Layout of a two-stage compressor consisting of multiple cells in each stage, check valves and pressure buffers. b) Schematic cross section of a single sorption cell with active heating and passive cooling by means of a gas-gap heat switch.

appears that ice crystallites form an obstruction in front of the restriction and by that impede the nitrogen flow from entering the restriction.

A literature research on the deposition of ice crystals at low temperatures and at low partial pressure of water vapor was performed. Different phases of ice can grow inside the microcooler. In the relevant temperature and pressure ranges, cubic ice and hexagonal ice are the phases that are most likely to occur.[10] These different phases of ice also have different thermal and mechanical stabilities. At this moment, more research is being performed on this topic to get a better understanding of the ice growing mechanisms inside a microcooler, and more importantly, on how to prevent clogging.

CLOSED CYCLE SORPTION COOLING

A small cryocooler without moving parts can be realized by combining a sorption compressor with a JT microcooler in a Linde-Hampson (LH) cooling cycle.[11] A sorption compressor consists of a number of independently functioning cells (Fig. 5). Each cell incorporates a container filled with a sorber and means to actively control the temperature of the container.

The low-pressure working fluid is adsorbed by the sorber at an ambient temperature and subsequently desorbed at a high pressure by heating the container. By manipulating the gas flows with passive check valves and thermally cycling the cells, a continuous flow can be maintained in the cooler. A valid extension to this simple approach is a two-stage compressor arrangement as shown in Fig. 5a. Here, the working fluid is first compressed from the low pressure to an intermediate pressure and then to the high pressure in the second stage[11]. Compared to a single-stage compressor, a two-stage compressor is more energy efficient and can generate a higher compression ratio. Adding buffers at all three pressure points helps achieve a stable gas flow, and can lead to a reduction of the number of cells in each stage and can lower the total power consumption of the compressor.

The thermal cycling of a cell is realized by means of active heating with a heater encapsulated within the container and passive cooling (Fig. 5b). The heat flow from the container to the environment is managed by a gas-gap heat switch placed between the container and the heat sink. The gas-gap heat switch can be readily controlled by placing a small heated sorber pill within the cavity of the gas-gap. Thermal cycling of this pill results in changes of the pressure of the gas in the gas-gap and thus its thermal conductivity.

Derking et al.[13] have calculated that methane is the most efficient working fluid for a JT cold stage operating at the target cooling temperature of 100 K. Here, this claim is further investigated to assess its validity when a whole sorption-based cooler working at room temperature is taken

Table 1. Comparison of three candidate working fluids for a cooler with 50 mW of cooling power at 100 K. T_{cool} is the cold-tip temperature; p_L and p_I are the low and intermediate pressures; T_{H1} and T_{H2} are the high temperatures of the 1st and 2nd stage; COP_{comp} is the COP of the compressor; COP_{tot} is the overall COP of the cooler including the compressor; $P_{in,\,I}$ and $P_{in,\,II}$ are the average input powers for the 1st and 2nd stage.

Fluid	T_{cool} (K)	P_L (bar)	P_I (bar)	T_{H1} (K)	T_{H2} (K)	COP_{comp} (%)	COP_{tot} (%)	$P_{in,I}$ (W)	$P_{in,\,II}$ (W)
nitrogen	100.4	8.00	24.0	425	455	1.446	0.107	24.1	22.5
carbon monoxide	100.1	5.50	19.2	445	485	1.340	0.104	24.7	23.3
methane	100.2	0.35	3.9	480	625	1.499	0.153	18.9	13.7

into consideration. To evaluate which of the fluids is the best from a compressor design perspective, the following aspects were analyzed:

- the thermodynamic efficiency of a compressor operating with a given fluid under optimum conditions, expressed in terms of the coefficient of performance (COP) of the compressor and the cooler[12],
- the dynamics of the compressor, where time needed to perform one compression cycle is assessed,
- the number of cells in the first and second stage required to meet the cooling power requirements, with both thermodynamic optimization and dynamic modeling results taken as inputs.

A quasi-static thermodynamic analysis of the cycle[12] was performed for carbon monoxide, methane and nitrogen as possible working fluid candidates for a sorption LH cooler delivering 50 mW of gross cooling power at 100 K at a high pressure of 80 bar. The baseline compressor design assumed a two-stage system with cylindrical cell containers of 10 cm in length and 1 cm in diameter. Saran activated carbon was chosen as the sorber material. The results are presented in Table 1 in which the operating points are optimized for maximum performance.

Dynamic modeling of the compressor shows that the gas-gap behavior greatly affects the performance of the cooler. Minimizing the time required to switch the thermal conductivity of the gas-gap and choosing the optimum gas-gap fluid and its operating pressures has a significant impact on both the power consumption and size of the compressor. Fig. 6 shows the influence of the gas-gap pressure in the *off* (low conductivity) state on the average input power to the compressor stages for hydrogen as the switching gas.

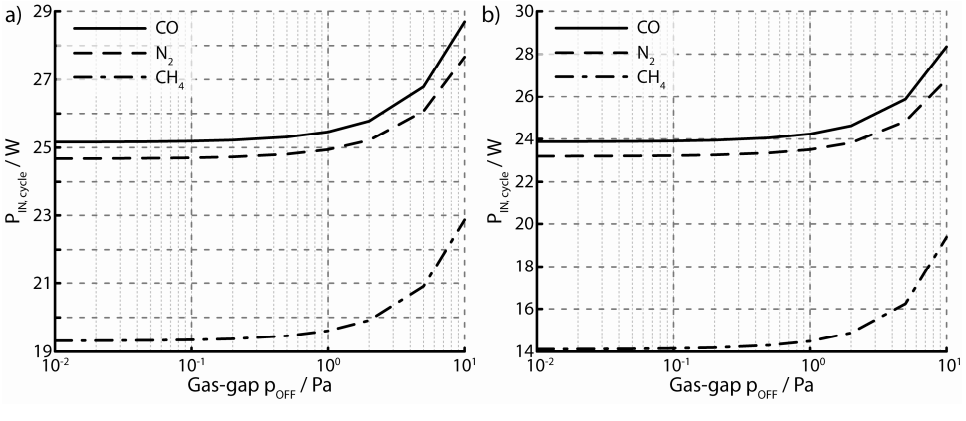

Figure 6. Average input power during a cycle to a) stage I and b) stage II for different working fluids as a function of the hydrogen pressure in the gas-gap in the low conductivity state.

Table 2. Minimum number of cylindrical cells in a sorption compressor stage based on dynamic modeling with the hydrogen gas-gap pressure in the *off* state, $p_{GG,\,Off}$ = 1 Pa and the hydrogen gas-gap pressure $p_{GG,On}$ during the cool-down phase indicated in the headers. The gas-gap width is set to either 100 μm or 250 μm.

gas-gap width	100 μm						250 μm					
$p_{GG,ON}$	100 Pa		200 Pa		400 Pa		100 Pa		200 Pa		400 Pa	
Stage	I	II	I	II	I	II	I	II	I	II	I	II
carbon monoxide	4	3	3	3	4	3	4	3	4	3	4	3
nitrogen	4	3	4	3	4	3	5	4	4	3	4	3
methane	3	2	2	1	2	1	3	2	3	1	3	1

The final design output, expressed as the number of cells in each stage of the sorption compressor required to achieve the goal of 50 mW at 100 K, is presented in Table 2. Comparison of the data collected in Table 1 and Table 2 indicates that methane is the best candidate as a working fluid both in terms of power and space efficiency. It should be possible to realize such a cooler with just three cylindrical sorption cells of 10 cm in length and 1 cm in diameter and the total input power of around 33 W.

CONCLUSIONS

A new run of single-stage JT microcoolers was developed and fabricated, consisting of two types: one designed with a gross cooling power of 40 mW, and the other with a gross cooling power of 180 mW at 100 K at a high pressure of 80 bar. The temperature profile along the length of the CFHX of both types was measured as well as their cooling power. At a mass-flow rate of 3.4 mg/s and a high pressure of 90 bar, a net cooling power of 26 mW was measured for the first cooler type. The net cooling power of the second type is measured to be 131 mW at a high pressure of 80 bar and a mass-flow rate of 15.6 mg/s. Furthermore, measurements with a microcooler in different orientations have shown that the influence of gravity on the performance of the microcoolers is negligible.

Clogging in the low-power microcooler was investigated. No clogging is occurring when the microcooler is driven by nitrogen gas cleaned with a microtorr® getter. However, when unpurified nitrogen gas (5.0) is used, clogging is observed during cool down and prevents the microcooler from cooling down below about 230 K.

Also, the combination of a JT micro cold stage with a sorption compressor was investigated. A design of such a cooler system that has a cooling power of 50 mW at 100 K is made on the basis of a quasi-static thermodynamic analysis. It is shown that methane is the best working fluid for such a cycle, both in terms of power and space efficiency. In this design, the sorption compressor consists of three cylindrical cells of 10 cm in length and 1 cm in diameter. The total input power of the cooler will be around 33 W.

ACKNOWLEDGMENT

The authors gratefully acknowledge the support of the Dutch Technology Foundation STW and the European Space Agency under Contract No. 20768/NL/EM.

REFERENCES

1. Burger, J.F., Holland, H.J., Seppenwoolde, J.H., Berenschot, E., ter Brake, H.J.M., Gardeniers, J.G.E., Elwenspoek, M., Rogalla, H., "165 K microcooler operating with a sorption compressor and a micromachined cold stage," *Cryocoolers 11*, Kluwer Academic/Plenum Publishers, New York (2001), pp. 551-560.
2. Lerou, P.P.P.M., Venhorst, G.C.F., Berends, C.F., Veenstra, T.T., Blom, M., Burger, J.F., ter Brake, H.J.M., Rogalla, H., "Fabrication of a micro cryogenic cold stage using MEMS-technology," *J. Micromech. Microeng.*, vol. 16 (2006), pp. 1919-1925.

3. Lerou, P.P.P.M., ter Brake, H.J.M., Burger, J.F., Holland, H.J, Rogalla, H., "Characterization of micromachined cryogenic coolers," *J. Micromech. Microeng.*, vol. 19 (2007), pp. 1956-1960.
4. Lerou, P.P.P.M., Veenstra, T.T., Burger, J.F., ter Brake, H.J.M., Rogalla, H., "Optimization of counterflow heat exchanger geometry through minimization of entropy generation," *Cryogenics*, vol. 45 (2005), pp. 659-669.
5. Chao, H.S., Lerou, P.P.P.M., Mudaliar, A.V., Holland, H.J., Derking, J.H., Zalewski, D.R., ter Brake, H.J.M., "Analysis of multi-stage Joule-Thomson microcoolers," *Cryocoolers 16*, ICC Press, Boulder, CO (2011), (this proceedings).
6. Saes Pure Gas Inc., San Luis Obispo, CA, USA, <www.saesgetters.com>, visited 28 April 2010.
7. Ansys Inc., *Fluent*, <www.fluent.com/>, visited 5 May 2010.
8. Lerou, P.P.P.M., ter Brake, H.J.M., Holland, H.J., Burger, J.F., Rogalla, H., "Insight into clogging of micromachined cryogenic coolers," *Appl. Phys. Lett.*, vol. 90 (2007), pp. 064102-1/3.
9. Derking, J.H., ter Brake, H.J.M., Sirbi, A, Linder, M., Rogalla, H., "On-chip detector cooling for space applications," *Cryocoolers 15*, ICC Press Boulder, Co, USA (2008), pp. 405-413.
10. Zheligovskaya, E.A., Malenkov, G.G., "Crystalline water ices," *Russ. Chem. Rev.*, vol. 75 (2006), pp. 57-76.
11. Wiegerinck, G.F.M., Burger, J.F., Holland, H.J., Hondebrink, E., ter Brake, H.J.M., Rogalla, H., "A sorption compressor with a single sorber bed for use with a Linde-Hampson cold stage," *Cryogenics*, vol. 46 (2006), pp. 9-20.
12. Wiegerinck, G.F.M., ter Brake, H.J.M., Burger, J.F., Holland, H. J., Rogalla, H., "Thermodynamic optimization of sorption-based Joule-Thomson coolers," *Cryogenics*, vol. 47 (2007), pp. 143-152.
13. Derking, J. H., ter Brake, H. J. M., Sirbi, A., Linder, M., Rogalla, H., "Optimization of the working fluid in a Joule-Thomson cold stage," *Cryogenics*, vol. 49 (2009), pp. 151-157.